Journal of Microscopy, Vol. 197, Pt 3, March 2000, pp. 219–223.
Received 27 September 1999; accepted 30 November 1999

SHORT COMMUNICATION

A wavefront generator for complex pupil function synthesis and point spread function engineering

M. A. A. NEIL, T. WILSON & R. JUŠKAITIS
Department of Engineering Science, University of Oxford, Parks Road, Oxford OX1 3PJ, U.K.

Key words. Aberration corrections, confocal microscopy.

Summary

We describe a simple method to produce an arbitrary complex optical field using a ferroelectric liquid crystal spatial light modulator. The system is configured so as to act as a pupil plane filter in a confocal microscope. The ability to tune the complex pupil function permits the system to be used both to modify the imaging performance by effectively engineering the point spread function as well as to remove optical aberrations present in the optical system.

Introduction

There are many instances in optical microscopy in which pupil plane filters are used to tune the imaging in some way so as to enhance the contrast or resolution of certain object features. Perhaps two of the most commonly employed are the annular ring required for dark-ground illumination and the absorbing annular phase ring of the Zernike phase contrast system (see, e.g. Pluta, 1988). Toraldo di Francia (1952) showed that by introducing a suitably designed array of concentric annular phase filters into the pupil plane of an objective lens an arbitrarily narrow amplitude point spread function would result. The advent of the confocal microscope, in which the effective point spread function is given by the product of the point spread functions of the two imaging lenses (Wilson, 1990), led to a renewed interest in the use of pupil plane filters in attempts to obtain superresolution (Hegedus, 1985; Hegedus & Sarafis, 1986; Pike *et al.*, 1990; Wilson *et al.*, 1990; Wilson & Hewlett, 1991). Other applications involve aberration correction (Sieracki & Hansen, 1995; Booth *et al.*, 1998). In all these cases it is necessary to design and construct filters to tune the amplitude and phase of the pupil function of the objective lens. It has been usual to accomplish this by introducing a physical filter into the system. In this short communication we shall present an alternative approach which uses a binary optical element, together with a technique developed from computer-generated holography (Lee, 1978), to produce an arbitrary complex field. This field may be used to modify the pupil function of an objective lens in the same way as a physical filter, but with the advantage of being rapidly reconfigurable.

Correspondence to: T. Wilson. Fax: +44 (0)1865 273905;
e-mail: tony.wilson@eng.ox.ac.uk

Methods and results

Our formal intention is to produce an arbitrary complex wave field, $a(x)\exp[j\phi(x)]$. We achieve this aim with the aid of the 4-*f* optical system (see, e.g. Goodman, 1968). In this system, which consists of two lenses separated by twice their focal lengths, a binary optical element, the pixels of which may be independently set to give a transmission of $+1$ or -1, is placed in the back focal plane of the first lens. The action of this first lens is to create the Fourier transform of the input field in the (Fourier) plane intermediate between the two lenses. A suitable spatial filter (pinhole) is then used to separate out part of this field, which is then Fourier transformed again by the second lens to give the desired output field. In order to understand the operation of the device we begin by considering a wavefront

$$f(x) = \exp(j[\phi(x) + \tau x]) \tag{1}$$

which contains the desired phase function $\phi(x)$ together with a linear phase tilt, τx. We shall present our analysis in one dimension for simplicity but the extension to two dimensions is routine. We now binarize the function, $f(x)$, according to the mapping shown in Fig. 1, which produces a binary wavefront, $g(x)$, depending on the value of $\phi(x) + \tau x$ and $\alpha(x)$. We shall return to the choice of $\alpha(x)$ later. The binarized wavefront, $g(x)$, may be described by the

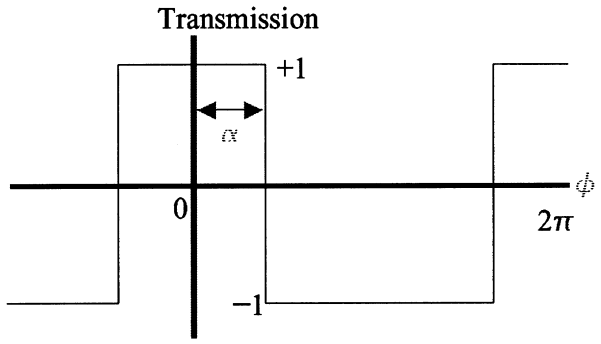

Fig. 1. The binarizing scheme showing that the transmission of the binary optical element is determined by the phase together with the angle, α.

Fourier series expansion

$$g(x) = \frac{4}{\pi}\left\{\frac{\alpha(x)}{2} - \frac{\pi}{4} + \sin(\alpha(x))\cos(\phi(x) + \tau x) + \frac{1}{2}\sin(2\alpha(x))\cos(2[\phi(x) + \tau x]) + \ldots\right\} \quad (2)$$

The action of the first lens is to produce a field $G(x_1)$ in the intermediate focal plane, x_1, given by the Fourier transform of $g(x)$, which may be written as

$$G(x_1) = \frac{2}{\pi}\left\{A(x_1) - \frac{\pi}{2}\delta(x_1) + [\Phi, (x_1 + \tau) + \Phi_1^*(\tau - x_1)] + [\Phi_2(x_1 + 2\tau) + \Phi_2^*(2\tau - x_1)] + \ldots\right\} \quad (3)$$

where $\delta(.)$ denotes the Dirac delta function and Φ_n represents the Fourier transform of $\sin(a\alpha(x))\exp[jn\phi(x)]$ and $A(x_1)$ is the Fourier-transform of $\alpha(x)$.

We now see that the effect of the tilt, τ, has been to position the diffracted orders at relative displacements of $\{+1, -1, +2, -2, \ldots\}$ from the axis. It is now a simple matter to isolate one of the first diffracted orders, say, $\sin(\alpha)\phi_1(x_1 - \tau)$, with a pinhole (spatial filter). Fourier transforming the transmitted light again with the second lens produces a field with amplitude $\sin(\alpha)$ and the desired phase, $\phi(x)$, together with the pre-applied tilt which may be easily removed by repositioning the second lens laterally. Thus, if we now consider the desired complex output field

$$a(x)\exp(j[\phi(x) + \tau x]) = u + jv \quad (4)$$

we conclude that we must binarize this field according to the phase mapping of Fig. 1 with the value of α determined by the amplitude, $a = (u^2 + v^2) = \sin(\alpha)$. It is now straightforward to combine these requirements into the simple phase mapping shown in Fig. 2 where we note that all complex numbers, $u + jv$, map within the circle $u^2 + v^2 = 1$ where the boundary between $+1$ and -1 modulation given by the semicircles $u^2 + (v \pm 1/2)^2 = 1/4$. We note that for the special case of phase only modulation, $a = 1$, $\alpha = \pi/2$, the modulation scheme reduces to that previously described by Neil *et al.* (1998) for producing an arbitrary phase front.

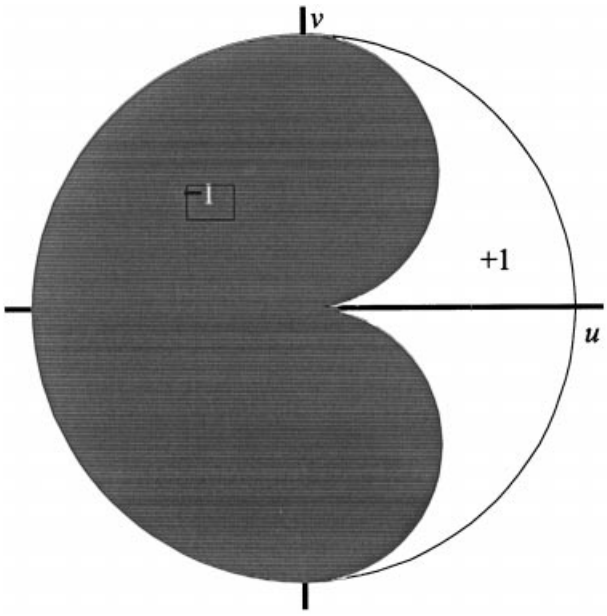

Fig. 2. The mapping of a complex field $u + jv$ into the required $+1$ or -1 phase modulation.

In order to implement the binary phase modulation in practice we elected to use a single ferroelectric liquid crystal spatial light modulator (FLCSLM) together with two suitably orientated polarisers in a reflection geometry (Neil *et al.*, 1998). This arrangement causes an incident plane wave to be reflected uniformly with a reduced intensity and a relative phase change of 0 or π depending on the state of the device. The FLCSLM we used consisted of a square array of 256×256 square pixels. This results, among other things, in aliasing due to pixellation, which means that higher diffracted orders can appear close to the desired first order in the Fourier plane. We choose the overall phase tilt to minimize these effects. Although our theory has been written for the one-dimensional case it is, as we have said, readily extendable to two dimensions. We have found that an overall tilt across the square aperture of 88π in the x-direction together with 120π in the y-direction is adequate to give good performance.

In order to demonstrate the versatility of this approach we constructed the system shown in Fig. 3. An expanded 488 nm laser beam is reflected by a polarizing beamsplitter onto the FLCSLM (a 256×256 by 15 μm square pixel silicon backplane device; Displaytech Model SLM 256P). Light which is reflected from the FLCSLM and passes through the same polarizing beamsplitter has a binary phase modulation determined by the pattern displayed on the FLCSLM. This field is then Fourier transformed by the first 180 mm focal length lens. A 2.5 mm diameter pinhole spatial filter is placed in the back focal plane of this lens to isolate the first diffracted

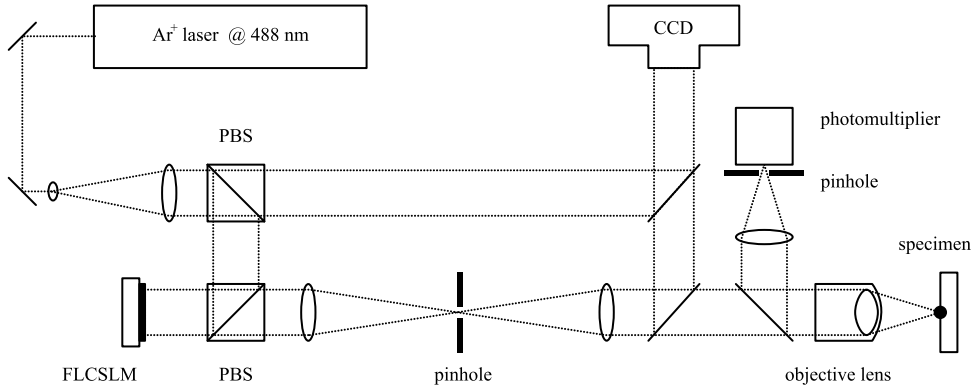

Fig. 3. Schematic diagram showing both the wavefront generator and its interface to the microscope system. PBS = polarizing beamsplitter; FLCSLM = ferroelectric liquid crystal spatial light modulator.

order as required. A second 180 mm lens is then used to Fourier transform the spatially filtered field to provide the desired complex output field, which is then used to tune the illuminating pupil function of the imaging lens in a confocal microscope. In order to demonstrate the versatility of our approach we also made provision for the inclusion of a reference beam so as to be able to record interferograms of the complex fields generated by the FLCSLM system.

We show in Fig. 4 a number of experimentally generated complex fields which were used to tune the pupil function of an objective lens in a number of desired ways. In all cases the left-hand image shows an interferogram of the complex pupil function. In order to measure the resulting intensity point spread functions in the focal plane of a 1.0 NA oil immersion objective lens, a sample consisting of 100 nm gold beads was scanned in the focal region and the scattered light was collected by the photomultiplier through an open pinhole. The resulting images are shown when the object is scanned in both the lateral x-y plane (centre images) and the axial x-z plane (right-hand images). The results in the first row correspond to the case of no pupil function apodization. The straight fringes in the interferogram, together with the intensity point spread function, confirm that the introduction of a FLCSLM into the system does not adversely affect the performance and that diffraction-limited imaging is maintained. The second row shows that the system is configured so as to generate an annular phase ring within a circular pupil function. The presence of the phase ring is shown clearly by the discontinuous jumps in the fringes in the interferogram.

An important application of the system is in the correction of aberrations introduced by focusing deep into thick specimens. The predominant aberration in this case is likely to be spherical aberration and so it is important to be able to 'pre-aberrate' the probe beam with an appropriate amount of aberration to counteract this effect. We show the ability of the system to generate spherical aberration in the third row of Fig. 4. The pupil functions we have generated so far have been phase-only. We finally show the ability of the system to produce complex amplitude and phase pupil functions in the bottom row of Fig. 4. The pupil function in this case is chosen to be $\sin(\pi\rho)\exp[j\theta]$, where ρ denotes the normalized radius and $\exp[j\theta]$ indicates a helical phase distribution. It is clear that this pupil function has zeros at the centre of the lens ($\rho = 0$) as well as at the edge ($\rho = 1$). The presence of the helical phase also ensures that the point spread function is zero on-axis and this can be seen in the annular nature of the intensity point spread function in Fig. 4. It is clear that such a beam has application for example in stimulated-emission depletion imaging techniques (Klar & Hell, 1999) and optical trapping.

Finally, in Fig. 5 we show a series of confocal fluorescence images of features in a fluorescent sheet. These images were obtained in the following way. First, the scanning of the confocal microscope was switched off and the FLCSLM configured so as to have an intensity point spread function corresponding to the scale bar and other features to be seen in Fig. 5. These features were photobleached into the fluorescent sheet, which had been created by writing a stripe on a microscope slide with a fluorescent marker pen. The scanning was then switched on and the FLCSLM reconfigured so as to provide no pupil function apodization (top row of Fig. 4) and the images of Fig. 5 recorded.

Conclusion

We have shown here that it is possible to configure a binary phase-only FLCSLM in such a way as to produce accurately any desired complex field so as, for example, to tune the pupil function of a confocal microscope. The system is versatile and readily reconfigurable. Unfortunately this is achieved at the expense of being relatively light inefficient. Although this is not a problem as far as tuning the pupil function of the first (illuminating) lens in a confocal microscope is concerned, it may be inappropriate to adopt this approach for the pupil function of the second

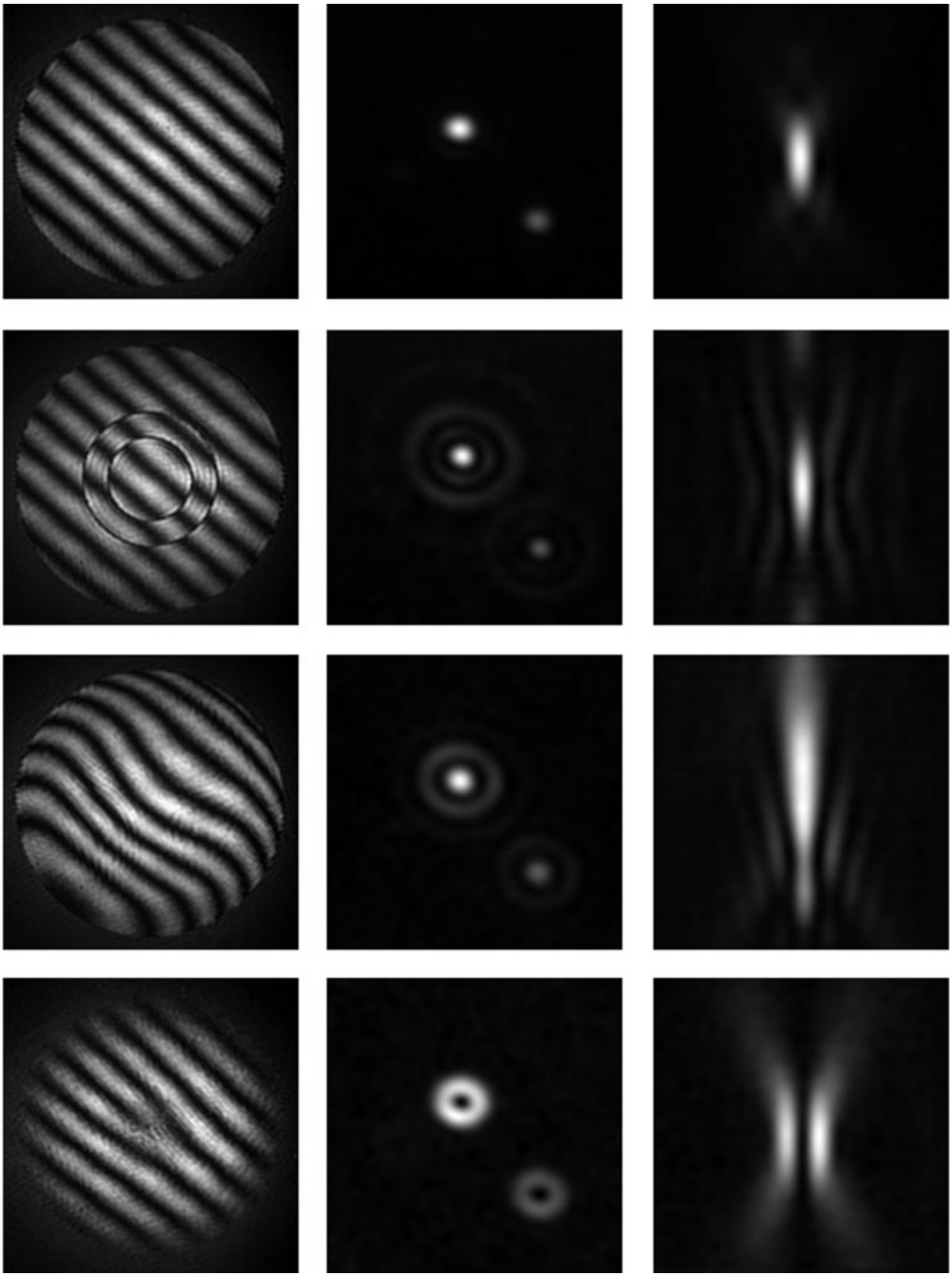

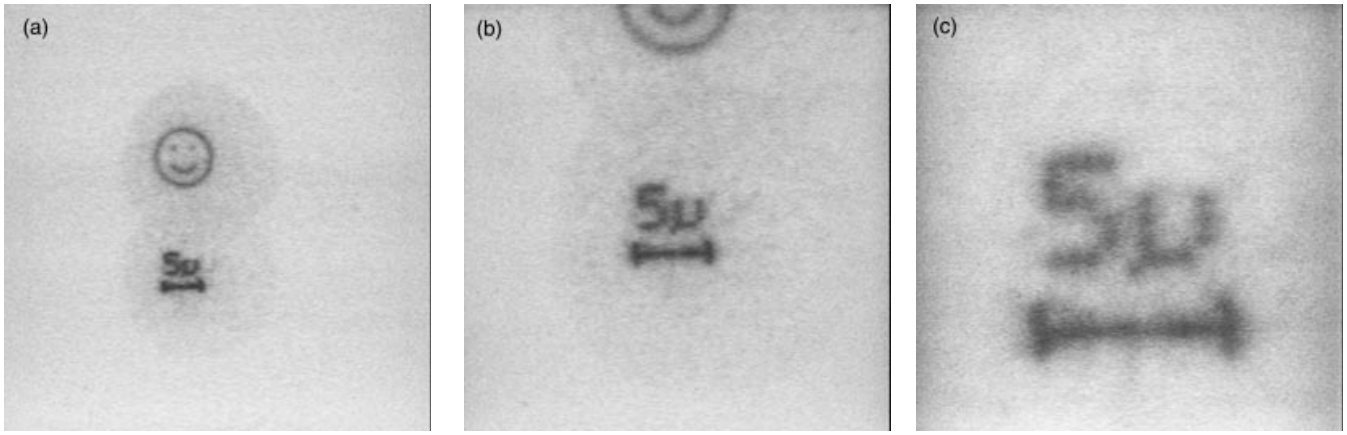

Fig. 5. Confocal images of a fluorescent sheet. The scale bar and other image details were photobleached into the specimen by the wavefront generator.

(detection) lens in very low signal level applications. However, this is thought to be a relatively minor drawback, as much can be achieved by modifying the pupil function of only one of the imaging objective lenses.

References

Booth, M.J., Neil, M.A.A. & Wilson, T. (1998) Aberration correction for confocal imaging in refractive index mismatched media. *J. Microsc.* **192,** 90–98.

Goodman, J.W. (1968) *Introduction to Fourier Optics*. McGraw-Hill, New York.

Hegedus, Z. (1985) Annular pupil arrays: application to confocal scanning. *Opt. Acta*, **32,** 815–826.

Hegedus, Z. & Sarafis, V. (1986) Super-resolving filters in confocally scanned imaging systems. *J. Opt. Soc. Am.* **A3,** 1892–1896.

Klar, T.A. & Hell, S.W. (1999) Subdiffraction resolution in far-field fluorescence microscopy. *Opt. Lett*, **24,** 954–956.

Lee, W.H. (1978) Computer-generated holograms; techniques and applications. *Progress in Optics* Vol. XVI (ed. by E. Wolf), pp. 121–232. Elsevier, New York.

Neil, M.A.A., Booth, M.J. & Wilson, T. (1998) Dynamic wave-front generation for the characterisation and testing of optical systems. *Opt. Lett*, **23,** 1849–1851.

Pike, E.R., Davis, R.E., Walker, J.G. & Young, M.R. (1990) An introduction to singular systems with application to confocal microscopy. *J. Microsc.* **160,** 107–114.

Pluta, M. (1988) *Advanced Light Microscopy.* Elsevier, Amsterdam.

Sieracki, C.K. & Hansen, E.W. (1995) Pupil function correction in 3D microscopy. *Proc. SPIE*. **2412,** 99–108.

Toraldo di Francia, G. (1952) Super-gain antennas and optical resolving power. *Nuovo Cimento*, Supplement **9,** 426–435.

Wilson, T. (1990) *Confocal Microscopy.* Academic Press, London.

Wilson, T., Hewlett, S.J. & Sheppard, C.J.R. (1990) Use of objective lenses with slit pupil functions in the imaging of line structures. *Appl. Opt*. **29,** 4705–4714.

Wilson, T. & Hewlett, S.J. (1991) Super-resolution in confocal scanning microscopy. *Opt. Lett*. **16,** 1062–1064.

Fig. 4. The left-hand columns show interferograms of the pupil function, together with their corresponding intensity point spread functions measured in the lateral x-y plane (centre column) and in the axial x-z plane (right-hand column). The first row corresponds to no apodization and the straight fringes indicate that the FLCSLM may be used without introducing unwanted aberrations. The second row shows the wavefront generator configured to produce an annular phase ring, as may be seen from the jump in the fringes. The third row simulates spherical aberration. Finally, the fourth row shows the ability to produce a complex wavefront consisting of a radial amplitude apodization, $\sin(\pi\rho)$, together with a helical phase variation. Note the annular nature of the intensity point spread function in this case.